

Document downloaded from:

<http://hdl.handle.net/10251/182266>

This paper must be cited as:

Carregari-Polachini, T.; Mulet Pons, A.; Telis-Romero, J.; Carcel, JA. (2021). Acoustic fields of acid suspensions containing cassava bagasse: Influence of physical properties on acoustic attenuation. *Applied Acoustics*. 177:1-10.
<https://doi.org/10.1016/j.apacoust.2021.107922>



The final publication is available at

<https://doi.org/10.1016/j.apacoust.2021.107922>

Copyright Elsevier

Additional Information

25 high correlation ($|r| > 0.87$ and $p_{\text{value}} \leq 0.05$) with experimental thermophysical properties
26 of the suspensions.

27 **Keywords:** acoustic fields, calorimetric method, ultrasound, attenuation, modelling.

28

29 **1. Introduction**

30 The second-generation (2G) ethanol appears as an interesting and alternative biofuel for
31 reducing the exploitation of non-renewable resources and for giving an eco-friendly
32 destination to the agro-industrial residues. Its production consists of biomass pretreatment
33 and hydrolysis, fermentation of the resulting sugars and ethanol distillation. However,
34 pretreatment and hydrolysis of biomass are the most challenging steps that should be
35 addressed to reduce the processing costs and make possible the bioethanol production
36 with good efficacy [1].

37 In order to reduce the feedstock costs, different residues from agroindustry can be
38 employed. Among them, cassava bagasse can be considered an interesting raw material
39 due to its rich composition of residual starch ($>30\%$ dry basis) and high availability in
40 countries as Brazil ($\sim 2,000,000$ tons of wet bagasse/year) (Polachini 2019a). Meanwhile,
41 the performance of each biomass under a given process needs to be evaluated separately
42 since their composition and structural arrangement can vary from one to another [2].
43 Similarly, the method used for treating these residues is of great importance for improving
44 the technological issues linked to the biofuel production. In addition to conventional
45 techniques, alternative and non-conventional ones such as microwave, CO₂ supercritical,
46 ozone and ultrasound application has been highlighted [3, 4].

47 Although high-intensity ultrasound (US) is a versatile technology, a special focus has
48 been given to its potential use for enhancing biomass conversion into bioethanol [5-7].
49 The sonication of biomass provides mechanical energy in the form of sound waves, which

50 produces a series of bubble collapses close to the solid-liquid interface. It is able to break
51 down the carbohydrate-lignin bonds, to depolymerize hemicellulose, cellulose and/or
52 starch into sugars of low molecular chain and, consequently, to increase the surface area
53 for further enzymatic treatment [8]. Those effects are enhanced if some catalyst, e. g.
54 alkali and acids, are used together with sonication.

55 The success of such processes assisted by US is dependent on its yield of conversion but
56 also on its reproducibility. Well-designed treatments can be adequately reproduced from
57 small to large scale. For this, calorimetric method is considered the most adequate tool
58 for measuring the real acoustic power transmitted to the medium from a given value of
59 nominal electrical power. It assumes that all acoustic energy is converted into heat as a
60 consequence of the collisions between the cavitation bubbles [9]. Such collisions
61 generates pressure gradients which can be measured by hydrophone and, then, correlated
62 with calorimetrically measured power [10]. But, the sensitivity of hydrophones to acids
63 and higher input power could raise difficulties on working with suspensions with constant
64 movement of particles. In this sense, calorimetric method can considered to be feasible
65 for reproduction in distinct systems with estimated standard deviation less than 10% [11].
66 This real acoustic power is the energy responsible by the actual sonochemical effects on
67 biomass, while the difference from the input electrical power is dispersed in form of wave
68 reflection back to the transducer, noise, heating and weariness of the ultrasonic processor,
69 etc [12, 13]. As seen as the sound waves suffer attenuation, the distance between the
70 sonotrode tip and the sample should be also taken into account for the knowledge about
71 the distribution of acoustic energy in the reactor [14]. It influences the correct positioning
72 of the samples and the homogeneous treatment of heterogeneous medium as suspensions
73 [15]. Gogate [16] highlighted the need of such data to understand the energy distribution
74 from an irradiating at a given input power.

75 The properties of the medium play an important role on how the ultrasound propagates
76 through the medium. Thermal properties relate the capacity of the medium for absorbing
77 energy and transferring it. On the other hand, density and viscous properties reflect the
78 resistance to the cavitation occurrence. Such properties, in turn, can vary according to
79 conditions of temperature, biomass loading and catalyst concentration in the suspension.
80 Thus, this work aimed at determining the acoustic parameters (acoustic power, intensity,
81 density and yield of power conversion) for suspensions composed by different acid
82 solutions (pH 3–7) and cassava bagasse concentration (2–10% w·w⁻¹), at different
83 distance from the sonotrode (1.5 – 5.5 cm) subjected to a range of nominal input power
84 (160–400 W). The results were used to estimate the attenuation coefficient as well as the
85 dependence of the acoustic parameters on the experimental physical properties of such
86 suspensions.

87

88 **2. Materials and Methods**

89 **2.1. Samples preparation**

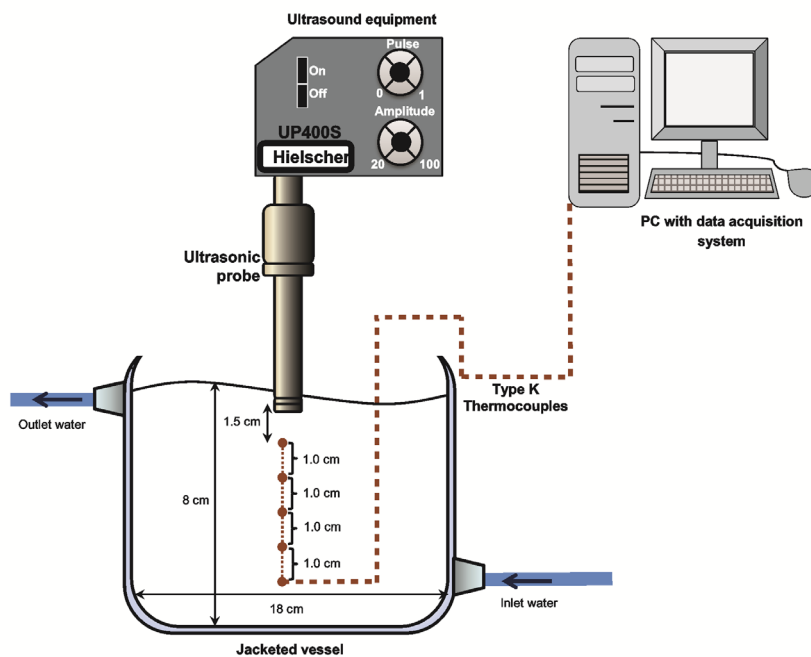
90 Dried and coarsely milled cassava (*Manihot esculenta*) bagasse was provided by
91 TechnoAmido (São Pedro do Turvo, São Paulo, Brazil) from the cassava starch extraction
92 process. The bagasse was then finely milled to obtain particle size lower than 0.147 mm
93 by a Tyler sieve mesh 100. This material was chemically and physically characterized in
94 the study of Polachini et al. (2019a).

95 Phosphoric acid (85% solution; Dinâmica, Diadema, São Paulo) was added to distilled
96 water to obtain acid solutions in the pH of 3.0; 4.0; 5.0; 6.0 and 7.0. Powdered cassava
97 bagasse was suspended in the acid solutions to obtain suspensions in the concentrations
98 of 2, 4, 6, 8 and 10% (g of cassava bagasse per 100 g of suspensions) at the different pH,
99 totaling 25 samples.

100

101 2.2. Acoustic field characterization

102 Acoustic parameters was determined by the calorimetric method, based on the
103 temperature increase of the suspensions in the first 90 s of ultrasound application in which
104 an adiabatic system is considered [17]. Temperature records were taken in the
105 experimental set-up shown in Figure 1. In this apparatus, it was used an ultrasonic
106 processor UP400S (Hielscher Ultrasonics GmbH, Germany) coupled with a titanium
107 sonotrode with diameter of 22 mm (model H40, Hielscher Ultrasonics GmbH, Germany),
108 operating at 24 kHz of frequency and maximum nominal input power of 400 W.



109

110 **Figure 1.** Apparatus used for the measurements of the acoustic fields produced on acid
111 suspensions of cassava bagasse.

112

113 Approximately 2 L of each one of the 25 suspensions were inserted in a jacketed stainless
114 steel chamber, and the samples were renewed for each analysis. The initial temperature
115 of the suspensions was maintained constant at 20 °C through a thermostatic bath (model

116 MA-184, Marconi, Piracicaba, Brazil). Five type J thermocouples were placed at different
117 position below the sonotrode: 1.5 cm, 2.5 cm, 3.5 cm, 4.5 cm and 5.5 cm, to be connected
118 to a data acquisition system (LabView 2010, National Instruments, USA). Measurements
119 were taken every 5 s over the ultrasound application. The experiments were varied
120 according to the percentage of the maximum nominal power P_N : 40% (160 W), 60% (240
121 W), 80% (320 W), 90% (360 W) and 100% (400 W).

122 Thus, the acoustic power could be calculated by the Eq. (1):

$$123 \quad P = V\rho c_p \frac{dT}{dt} \quad (1)$$

124 where P is the acoustic power (W), V is the volume of suspensions used in each
125 experiment (m^3), ρ is the suspension density ($\text{kg}\cdot\text{m}^{-3}$), c_p is the specific heat of the acid
126 suspensions ($\text{J}\cdot\text{kg}^{-1}\cdot^\circ\text{C}^{-1}$) and dT/dt heating rate ($^\circ\text{C}\cdot\text{s}^{-1}$). Density and specific heat of the
127 suspensions were acquired from the study of Polachini et al. (2019a) and the heating heat
128 was obtained by the linear regression between the temperature increase over the
129 sonication time.

130 Acoustic intensity (I , $\text{W}\cdot\text{cm}^{-2}$), acoustic density (D ; $\text{W}\cdot\text{mL}^{-1}$) and acoustic power per mass
131 of particles (D_p , $\text{W}\cdot\text{kg}^{-1}$ of cassava bagasse) were given by the Eq. (2), Eq. (3) and Eq.
132 (4), respectively:

$$133 \quad I = \frac{P}{A} \quad (2)$$

$$134 \quad D = \frac{P}{V} \quad (3)$$

$$135 \quad D_p = \frac{P}{V\rho w_s} \quad (4)$$

136 where A is the area of the transversal section of the sonotrode (cm^2) and w_s is the biomass
137 fraction in the suspension ($X_s/100$).

138

139 **2.3. Attenuation factor**

140 Acoustic field affects differently a product according to its distance from the sonotrode.

141 As seen it, acoustic intensity were correlated to the distance from the sonotrode by the

142 exponential relation (Eq. (5)) as presented by Mamvura et al. [18]:

$$143 \quad I = I_0 \exp(-2\alpha d) \quad (5)$$

144 where I_0 ($\text{W}\cdot\text{cm}^{-2}$) is the pre-exponential factor, α is the attenuation factor (cm^{-1}) and d is

145 the vertical distance (cm) from the sonotrode tip.

146

147 **2.5. Statistical evaluation and mathematical modeling**

148 The significant effects ($p_{\text{value}} < 0.05$) among the linear and quadratic effect of the pH of

149 the solution, solids concentration in the suspensions (X_S , % w·w⁻¹), nominal input power

150 (P_N , W) and distance of the sonotrode (d , cm) on the dT/dt , acoustic power P , acoustic

151 intensity I , acoustic density D , acoustic power per mass of particles D_p and yield of power

152 conversion acoustic power P (W) was evaluated using the software STATISTICA 10.0

153 (StatSoft Enterprise, Tulsa, USA). Polynomial equations, based on the Equation (6),

154 could be obtained for as a function of the significant parameters.

$$155 \quad \phi = \beta_0 + \beta_1 pH + \beta_2 pH^2 + \beta_3 X_S + \beta_4 X_S^2 + \beta_5 P_N + \beta_6 P_N^2 + \beta_7 d + \beta_8 d^2 \quad (6)$$

156 Where ϕ is the studied variable (P , I , D , D_p and Yield) and $\beta_0, \beta_1, \beta_2, \beta_3, \beta_4, \beta_5, \beta_6, \beta_7$, and

157 β_8 are empirical parameters of the polynomial model.

158 Graphical plot and non-linear regressions were carried out through the software OriginPro

159 8.0 (OriginLab Corporation, Northampton, USA). The accuracy of the obtained models

160 was expressed by the determination coefficient R^2 and by the root mean square error

161 ($RMSE$).

162

163 **2.5. Correlation between acoustic and physical properties**

164 As it is known that acoustic properties are dependent on the physical properties of the
165 medium, it was evaluate the correlation between acoustic intensity and physical properties
166 of the acid suspensions containing cassava bagasse. Among the physical properties, there
167 are apparent viscosity (Polachini et al., 2019b), density, thermal conductivity and thermal
168 diffusivity (Polachini et al., 2019a). A good agreement between acoustic intensity and a
169 given physical property was evidence by a Pearson correlation coefficient r close to 1 and
170 $p_{\text{value}} \leq 0.05$, considered significant at 95% of confidence.

171

172 **3. Results and discussions**

173 **3.1. Acoustic properties**

174 The ultrasound application over the 90 s of treatment resulted in a linear increase of
175 temperature ($R^2 > 0.968$) for all acid suspensions at the different positions of the
176 thermocouple. The slope dT/dt , corresponding to the linear variation of temperature
177 during ultrasound application, differs from 0.0063 to 0.0326 $^{\circ}\text{C}\cdot\text{s}^{-1}$ according to the pH,
178 solids concentration, nominal input power and distance from the sonotrode in the range
179 of studied conditions. Making use of the experimental heating rates together with the
180 density and specific heat of the acid suspensions (Polachini et al., 2019), acoustic power
181 could be calculated for all conditions using Equation (1). These values were in the range
182 between 49.05 and 260.64 W.

183 Other acoustic parameters could be calculated from the acoustic power values. Depending
184 on the application system, one can be more practical than other. Therefore, acoustic
185 intensity was determined, resulting values between 12.90 and 68.57 $\text{W}\cdot\text{cm}^{-2}$. These values
186 are in the range ($< 100 \text{ W}\cdot\text{cm}^{-2}$) recommended by Gogate and Pandit [14], where the level
187 of power applied does not influence negatively the acoustic intensity as a consequence of

188 the cavitation bubble overgrowth and the subsequent decrease on the bubble wall
189 pressure.

190 Although acoustic density varied from 24.53 and 130.32 kW·m⁻³, another way to correlate
191 the acoustic properties with the sonochemical effects generated on the particles in the
192 suspension is to express acoustic power per mass of biomass. This acoustic density
193 reached 6.66 kW·kg of cassava bagasse⁻¹ while the lowest value was 0.24 kW·kg of
194 cassava bagasse⁻¹.

195 Understanding how each factor affects the acoustic property can provide important
196 information for the correct design of different processes assisted by ultrasound. The
197 influence of each variable (pH, solids concentration, nominal input power and distance
198 from the sonotrode tip) on the acoustic parameters was studied separately in the following
199 sections:

200

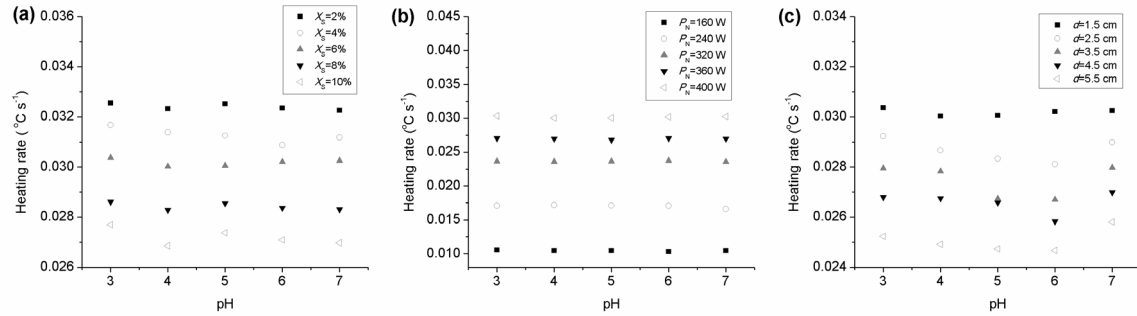
201 **3.1.1. Influence of pH on the acoustic properties**

202 The analysis of the estimated effects promoted by each variable on the heating heat was
203 firstly carried out. Variations in the pH of the solutions did not present significant
204 relationship ($p_{\text{value}} > 0.05$) with the heating rate. It indicated that altering the pH in the
205 interval between 3.0 and 7.0 was not significantly enough to promote different levels of
206 cavitation, in a similar way as observed for acid suspensions containing powdered peanut
207 shells [19]. Figure 2 reinforces that no clear trend could be seen for the heating rate at
208 different pH, i. e., suspensions containing biomass can be slightly acidified in order to
209 obtain optimal conditions for a possible enzyme actuation without significant alterations
210 on the cavitation activity, which could led to enzyme inactivation.

211 It was observed for all suspensions under the different nominal input power at any
212 position from the sonotrode. From this point, pH was not taken into account for

213 determining and modelling the following acoustic properties and their dependence by the
 214 solids concentration, nominal input power and distance from the sonotrode tip at a fixed
 215 pH of 7.0.

216



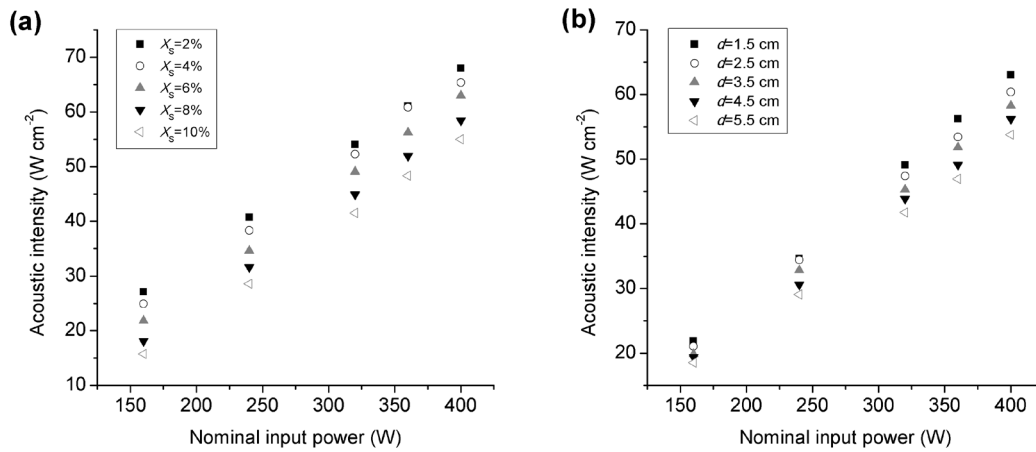
217

218 **Figure 2.** Heating rate as affected by pH at different (a) solids concentration ($P_N=400$ W
 219 and $d=1.5$ cm), (b) nominal input power ($X_S=6\%$ and $d=1.5$ cm) and (c) distances from
 220 the sonotrode ($X_S=6\%$ and $P_N=400$ W).

221

222 3.1.2. Influence of P_N on I

223 Positive variations in the nominal electrical power caused linear increase in the heating
 224 rate, and consequently in the acoustic intensity ($p_{\text{value}} < 0.05$). This linear dependence was
 225 previously reported for different systems in literature for different solvents [20, 21],
 226 distilled water [18], municipal wastewater with suspended particles [22] and peanut shell
 227 suspensions [19]. Increasing the nominal applied energy enhanced the heating rate in the
 228 suspensions, which tended to increase the acoustic intensity in all the suspensions at the
 229 different points of measurement (Figure 3). The increase in the electrical input power
 230 could have increased the acoustic intensity by the generation of a more violent collapse
 231 between cavitation bubbles [23]. Moreover, the differences of the slope and intercept of
 232 the curves may be attributed to the efficiency of energy conversion at different electrical
 233 power in the varied conditions [21].



235

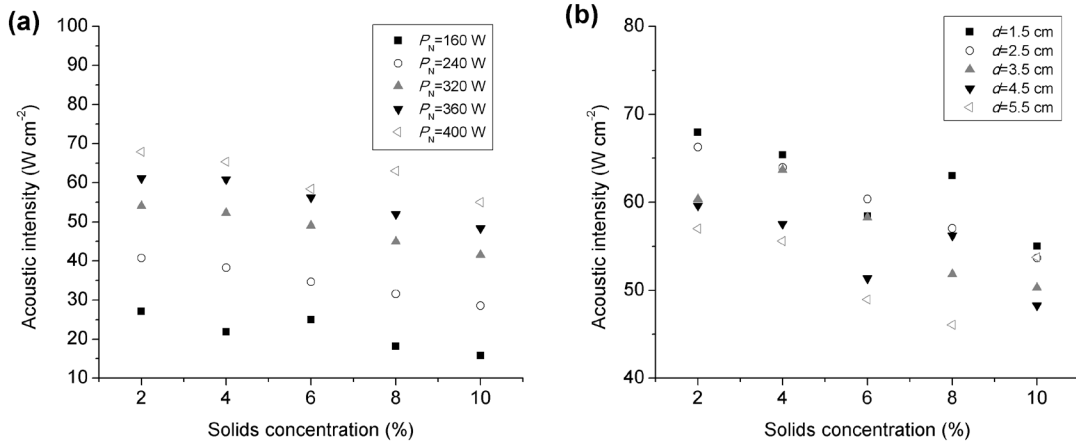
236 **Figure 3.** Acoustic intensity I ($\text{W}\cdot\text{cm}^{-2}$) as affected by the nominal input power at (a)
 237 different solids concentration ($d=1.5$ cm) and (b) different distances from the sonotrode
 238 ($X_s=6\%$).

239

240 3.1.3. Influence of X_s on I

241 A significant linear and quadratic effect ($p_{\text{value}} < 0.05$) was observed by the solids
 242 concentration on the heating rate. The increase in the solids content resulted lower heating
 243 rates, probably due to the higher viscosity of concentrated suspensions in comparison to
 244 dilute ones (Polachini et al, 2019b). Consequently, higher acoustic intensity was observed
 245 for the more diluted suspensions at the higher amplitude of nominal input power in the
 246 closer position to the tip (Figure 4). The presence of suspended particles promotes the
 247 energy attenuation, as higher energy levels are required to overcome the molecular
 248 interaction in the decompression zones during sound wave propagation. Same behavior
 249 was evidenced in a previous studied, where powdered peanut shells was suspended in
 250 water [19]. In addition, the reduced acoustic intensity in suspensions with higher
 251 concentrations of cassava bagasse may be attributed to the difference between the liquid

252 and particle impedance. As the ultrasound propagates through the medium and come
 253 across a particle, it is expected the reflectance and scattering of acoustic fields [24, 25].
 254



255
 256 **Figure 4.** Acoustic intensity I ($\text{W}\cdot\text{cm}^{-2}$) as affected by solids concentration (a) under
 257 different nominal input power ($d=1.5$ cm) and (b) at different distances from the
 258 sonotrode ($P_N=400$ W).

259

260 3.1.4. Influence of d on I

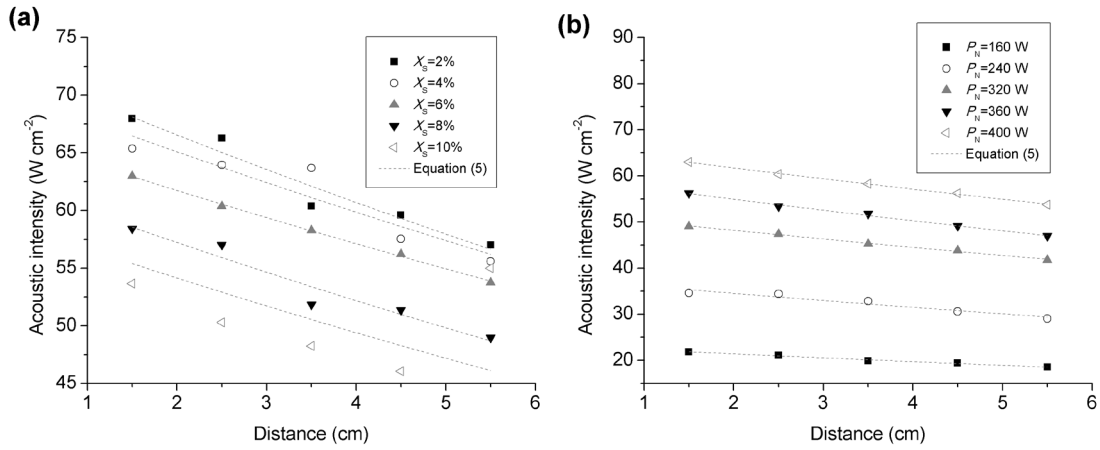
261 It could be observed the acoustic intensity decreased if measurements are taken away
 262 from the probe, evidencing that energy attenuation occurs through the material during
 263 sonication (Figure 5). Possible reasons for this attenuation are related to the reflection,
 264 refraction, diffraction or scattering of the wave or even as a result of the viscous
 265 interactions that degrade the acoustic energy into heat [18, 26].

266 Although acoustic intensity showed to be linearly dependent on the distance from the tip
 267 increased ($p<0.05$), I is commonly correlated with d by an exponential relation. It allows
 268 the estimation of the attenuation factor (α) and the pre-exponential term (I_0) contained in
 269 the Equation (5).

270 In this sense, acoustic intensity values for all suspensions under different input power
 271 levels were plotted against the distance from the tip of the sonotrode and fitted to Equation

272 (5) (Figure 5). The fitting procedure resulted good accuracy ($R^2>0.8416$ and $RMSE<1.79$),
273 presenting close agreement of the predicted values with the observed ones (Table 1).
274 From the analysis of variance, the pre-exponential term (I_0) demonstrated to be dependent
275 on the cassava bagasse concentration and on the input power ($p<0.05$). It tended to
276 increase with decreasing solids concentration and increasing input power. On the other
277 hand, attenuation factor (α) did not present a significant relationship with these variables.
278 All values of acoustic intensity are supposed to be in the region of linear decrease of the
279 exponential equation (Figure 5), leading to the absence of correlation of α with X_S and P_N
280 with a constant mean attenuation value of 0.021 cm^{-1} for the conditions applied to the
281 suspensions. The constant $\alpha/(\text{frequency})^2$, considered unique for each solution [27], can
282 be so determined as a constant value $3.64 \times 10^{-11} \text{ cm}^{-1} \cdot \text{s}^2$ for the studied suspensions. Even
283 more, the distance of half-acoustic intensity in which acoustic intensity decreases by 50%
284 ($-\log(I/I_0)$) would be assumed equal to approximately 11.8 cm. This value is lower than
285 the ones observed by Son et al. [27] for tap water at higher frequency than 35 kHz,
286 indicating that suspended particle of cassava bagasse could have actuated as attenuating
287 material in contrast to pure water. Analogously, the constant $\alpha/(\text{frequency})^2$ was higher
288 in this study when comparing with the previous authors, leading to the same observation.
289 When measuring acoustic pressure by indirect methods, Chivate and Pandit [28] found
290 that the zone of exponential decrease of pressure was found below 1 cm from the
291 sonotrode, almost touching it. In other words, it is probable that acoustic intensity
292 decreased in a constant way from 1.5 cm up to 5.5 cm away from the sonotrode because
293 the maximum acoustic intensity decreased exponentially when too little distances close
294 to the tip are taken. Mamvura et al. [18] and Son et al [27] also reported similar linear
295 trend when applying electrical power above 100 W in distilled water over higher
296 distances. Therefore, concerning the design reactors for heterogeneous systems,

297 calculations about the acoustic intensity could be done considering that acoustic intensity
 298 would not suffer abrupt decreases, characteristic of exponential behavior, in the region
 299 between 1.5 and 5.5 cm.



300
 301 **Figure 5.** Acoustic intensity I ($W \cdot cm^{-2}$) as affected by the distance from the sonotrode at
 302 different (a) solids concentration ($P_N=400W$) and (b) nominal input power ($X_s=6\%$); data
 303 are fitted to the Equation (5).

304
 305 **Table 1.** Fitted values for I_0 and α at different input power and cassava bagasse
 306 concentrations.

P (W)	Parameters	Solids concentration, X_s (%)				
		2	4	6	8	10
160	I_0 ($W \cdot cm^{-2}$)	29.16	26.67	23.23	19.28	16.94
	α ($W \cdot cm^{-1}$)	0.0208	0.0228	0.0205	0.0171	0.0221
	R^2	0.9435	0.9894	0.9921	0.9557	0.9152
	$RMSE$	0.46	0.19	0.13	0.22	0.35
240	I_0 ($W \cdot cm^{-2}$)	43.66	40.98	37.85	33.99	30.55
	α ($W \cdot cm^{-1}$)	0.0202	0.0205	0.0229	0.0198	0.0204
	R^2	0.9858	0.9599	0.9577	0.9723	0.9686
	$RMSE$	0.32	0.52	0.55	0.34	0.34
320	I_0 ($W \cdot cm^{-2}$)	57.79	57.41	52.20	48.26	44.15
	α ($W \cdot cm^{-1}$)	0.0200	0.0229	0.0199	0.0207	0.0194
	R^2	0.9544	0.8426	0.9977	0.9561	0.9660
	$RMSE$	0.77	1.78	0.15	0.65	0.49
360	I_0 ($W \cdot cm^{-2}$)	65.71	65.43	60.02	55.83	52.12
	α ($W \cdot cm^{-1}$)	0.0230	0.0230	0.0221	0.0235	0.0227
	R^2	0.9536	0.9536	0.9962	0.9679	0.9794

	<i>RMSE</i>	0.99	0.99	0.24	0.71	0.51
	I_0 (W·cm ⁻²)	72.99	70.79	66.73	62.76	59.35
400	α (W·cm ⁻¹)	0.0230	0.0210	0.0194	0.0230	0.0229
	R^2	0.9634	0.9184	0.9988	0.9601	0.9906
	<i>RMSE</i>	0.98	1.36	0.13	0.88	0.39

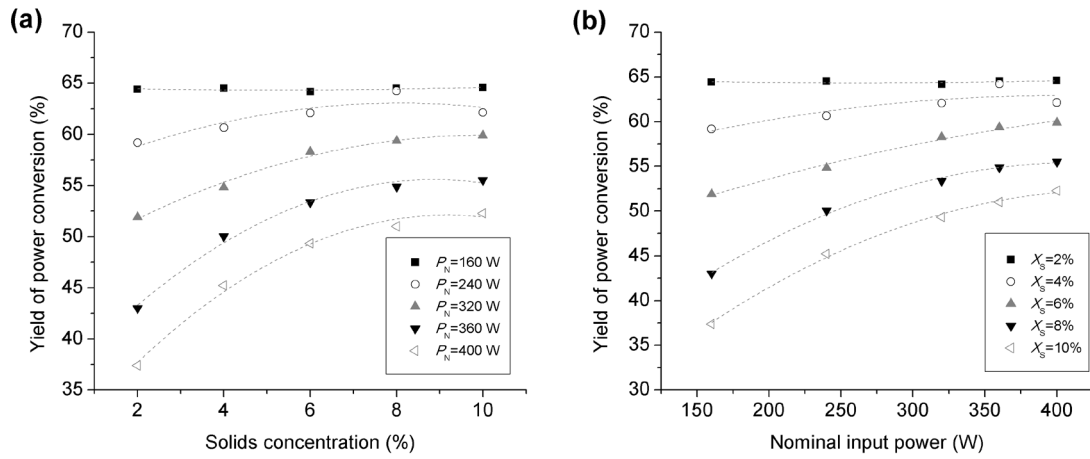
307

308 3.1.5. Conversion yield

309 Yield of power conversion is useful not only from an economical point of view but also
310 for designing appropriate ultrasonic processors to produce a given acoustic effect from
311 specific electrical input power. In the treatments of cassava bagasse by US, an
312 improvement of the conversion of electrical into acoustic energy was obtained as the
313 solids content decreased and the input power increased, attaining a maximum of 65.55%
314 in the studied conditions at the closer position to the tip. Löning et al. [13] and Polachini
315 et al. [19] reported close conversion yield values in similar conditions for water and
316 peanut shell suspensions, respectively. In the same point, yield could decrease to 36.81%
317 if the solids concentration is increased to 10% and nominal power was established at the
318 minimum value of 160 W. McDonnell et al. [29] also found better conversion rates when
319 operating ultrasound at higher nominal power, indicating that sonochemical effects are
320 supposed to be more intense at highest nominal power. Although it is not always
321 evidenced, Gibson et al. [22] and Polachini et al. [19] found that the efficiency of power
322 conversion increased non-linearly with nominal power when studying biomass
323 suspensions, which approached to a plateau level at higher P_N . Cárcel et al. [30] also
324 found a non-linear trend for sucrose solution, emphasizing that electrical input power
325 does not provide enough information about the actual acoustic intensity transmitted to the
326 medium. Similarly, a non-linear increase was observed in this study as the cassava
327 bagasse concentration increased, reaching a plateau above approximately 8% (Figure 6).
328 Such deviations from linearity are more noticeable both at higher nominal powers and
329 solids concentration. It highlights that controlling of the operations conditions and reactor

330 design can provide the required energy with the maximum efficiency of energy
 331 conversion [21, 26].

332



333

334 **Figure 6.** Yield of power conversion measured at the point of maximum cavitation ($d=1.5$
 335 cm) as a function of (a) nominal input power and (b) solids concentration.

336

337 3.2. Mathematical modelling

338 Acoustic properties can be predicted by both empirical and theoretical models. The
 339 obtained values for acoustic power, intensity, density and acoustic power per mass of
 340 particles could be fitted with good accuracy to polynomial equations in order to provide
 341 ready-to-use information for reproducing a given condition. Table 2 shows the fitting
 342 parameters of each corresponding acoustic variable.

343

344 **Table 2.** Fitting parameters of the Equation (6) for heating rate (dT/dt) acoustic power
 345 (P), acoustic intensity (I), acoustic density (D), acoustic power per mass of particles (D_p)
 346 and yield of power conversion.

Parameter	$\frac{dT}{dt}$ ($^{\circ}\text{C}\cdot\text{s}^{-1}$)	P (W)	I ($\text{W}\cdot\text{cm}^{-2}$)	D ($\text{kW}\cdot\text{m}^{-3}$)	D_p ($\text{kW}\cdot\text{kg}^{-1}$)	Yield (%)
β_0	4.03×10^{-3}	34.85	9.17	17.42	5.18	54.32
B_1	-	-	-	-	-	-

B_2	-	-	-	-	-	-
B_3	-4.81×10^{-4}	-4.04	-1.06	-2.02	-1.45	-1.57
B_4	-1.21×10^{-5}	-0.13	-0.03	-0.06	0.08	-0.04
B_5	7.49×10^{-5}	0.59	0.15	0.29	6.91×10^{-3}	0.09
B_6	-	-	-	-	-	1.19×10^{-3}
B_7	-8.54×10^{-4}	-6.75	-1.77	-3.37	-0.08	-2.24
B_8	-	-	-	-	-	-
R^2	0.9923	0.9921	0.9921	0.9921	0.9198	0.9199
$RMSE$	6.32×10^{-4}	4.87	1.28	2.43	0.45	2.11
EMR (%)	2.90	2.99	4.45	3.50	32.78	4.30

347

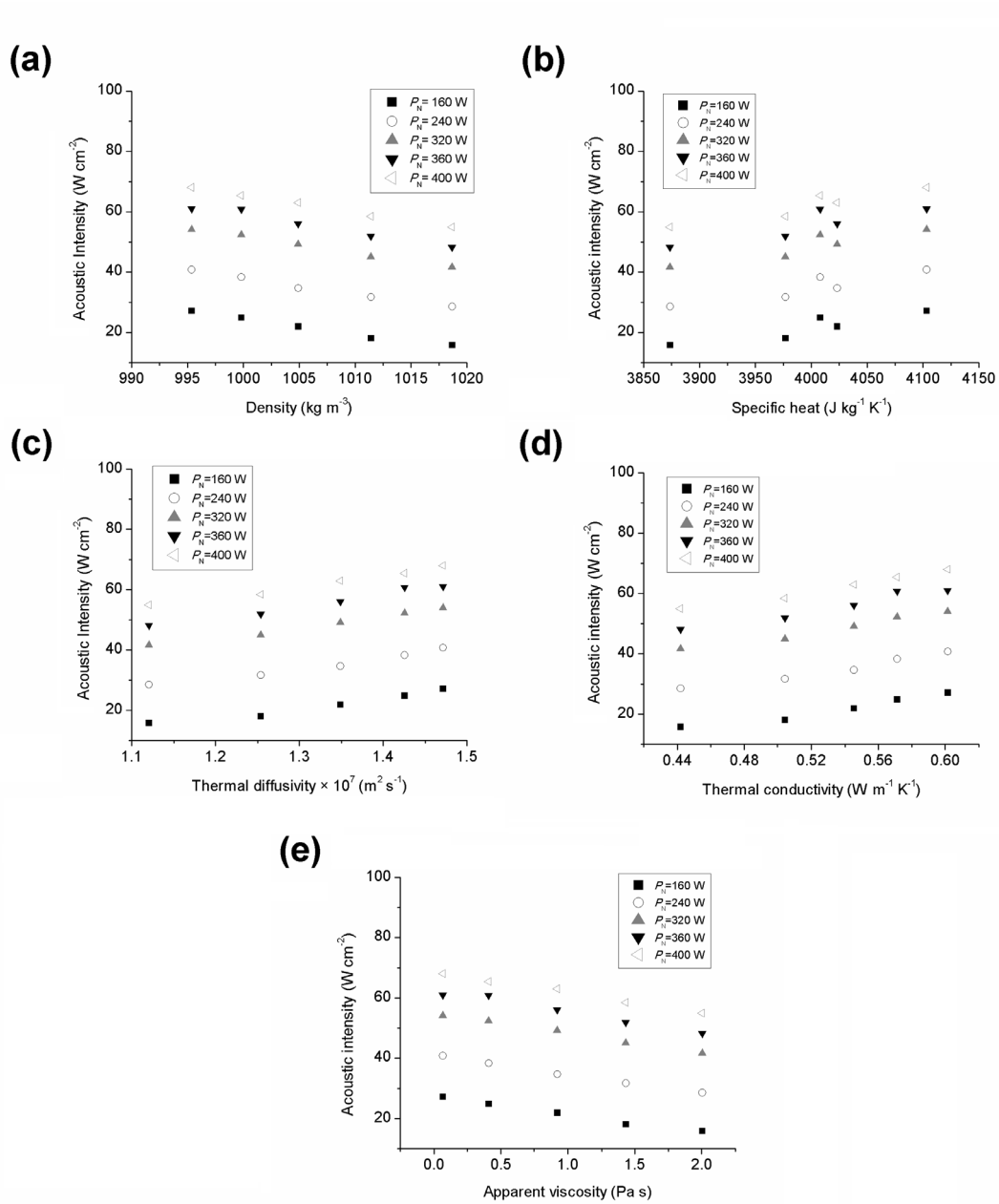
348 3.3. Correlation between acoustic and physical properties

349 Physical properties of the medium are supposed to affect the cavitation degree. In this
350 sense, acoustic intensity were correlated with experimental values of density (ρ), specific
351 heat (c_p), thermal diffusivity (α), thermal conductivity (λ) and apparent viscosity at fixed
352 shear rate of 10 s^{-1} ($\eta_{app,10s^{-1}}$) in the temperature of 25 °C.

353 All of the physical properties showed to be highly correlated with the acoustic intensity,
354 with $p_{\text{value}} \leq 0.05$ and high Pearson's correlation coefficient (Table 3). As expected,
355 acoustic intensity was strongly influenced by c_p and ρ since these properties are embedded
356 in the calculation of acoustic power from heating rate data. As the specific heat capacity
357 of the medium is increased and the density is decreased, the acoustic intensity is supposed
358 to increase (Figure 7a and 7b). The thermal properties (thermal diffusivity and thermal
359 conductivity) of the medium influenced positively the resulting values for acoustic
360 intensity, indicating that higher cavitation occurs more intensely in fluids with higher α
361 and λ (Figure 7c and 7d). On the other hand, suspensions with increased viscosity
362 presented lower acoustic intensity as characterized by the negative correlation coefficient
363 (Figure 7e). Toma et al. [21] observed that solvents with elevated viscosity seemed to
364 present lower acoustic power, similarly as noticed for cassava bagasse. According to Raso
365 et al. [17], the molecular motion is reduced in liquids with higher viscosity, i. e. more

366 energy is required by the molecules to overcome the critical molecular distance necessary
 367 to induce the formation of cavitation bubbles.

368



369

370 **Figure 7.** Acoustic intensity (I) as a function of (a) density, (b) specific heat, (c) thermal
 371 diffusivity, (d) thermal conductivity and (e) apparent viscosity of the suspensions under
 372 different nominal input power (P_N).

373

374 **Table 3.** Parameters of Pearson correlations between acoustic intensity and each physical
 375 property in the different nominal input power at the closest position to the sonotrode.

P_N (W)	Parameter	Physical Property				
		ρ	c_p	α	λ	$\eta_{app,10s^{-1}}$
160	r	-0.9940	0.9099	0.9837	0.9798	-0.9965
	p_{value}	5.5×10^{-4}	3.2×10^{-2}	2.5×10^{-3}	3.4×10^{-3}	2.52×10^{-4}
240	r	-0.9944	0.9150	0.9843	0.9811	-0.9977
	p_{value}	5.0×10^{-4}	2.9×10^{-2}	2.3×10^{-3}	3.1×10^{-3}	1.3×10^{-4}
320	r	-0.9975	0.9168	0.9939	0.9893	-0.9979
	p_{value}	1.5×10^{-4}	2.8×10^{-2}	5.6×10^{-4}	1.3×10^{-3}	1.1×10^{-4}
360	r	-0.9868	0.8774	0.9877	0.9769	-0.9895
	p_{value}	1.8×10^{-3}	5.0×10^{-2}	1.6×10^{-3}	4.2×10^{-3}	1.3×10^{-3}
400	r	-0.9978	0.9353	0.9926	0.9916	-0.9963
	p_{value}	1.2×10^{-4}	2.0×10^{-2}	7.7×10^{-4}	9.3×10^{-4}	2.7×10^{-4}

376

377 4. Conclusions

378 The application of ultrasound in acid suspensions containing cassava bagasse resulted in
 379 different heating rates (from 0.0063 up to 0.0326 °C·s⁻¹) in the first seconds of sonication,
 380 being significantly enhanced by decreasing the solids concentration in the suspensions
 381 and increasing nominal input power, without significant influence of the pH in the studied
 382 conditions. It also demonstrated to be less intense as the measurements are taken away
 383 from the sonotrode tip, evidencing that attenuation occurred. This type of observation
 384 also reinforces the need by agitating suspensions for a homogeneous treatment.

385 From the values of heating rates, acoustic intensity could be determined in the range of
 386 12.90 and 68.57 W·cm⁻², following the same dependence on the studied variables as
 387 presented by the heating rate. Acoustic power, acoustic density and acoustic density per
 388 mass of particles could be also obtained. They were all well-fitted to polynomial models,
 389 presenting good accuracy ($R^2 > 0.9198$) in order to make available ready-to-use

390 information. The evaluation and modelling of acoustic intensity at different positions
391 from the sonotrode provided interesting data about the attenuation, which showed a
392 constant attenuation factor of $0.021 \pm 0.002 \text{ cm}^{-1}$ for any suspensions in the range of
393 studied conditions with distance of half-acoustic intensity approximately equal to 11.8
394 cm..

395 Additionally, acoustic intensity was well correlated ($|r| > 0.87$ and $p_{\text{value}} \leq 0.05$) with some
396 physical properties of the suspensions containing cassava bagasse. It tended to increase
397 in suspensions with increased thermal properties (specific heat capacity, thermal
398 diffusivity and thermal conductivity) and decreased density and viscosity. In this sense,
399 cavitation and, consequently the sonochemical effects on the biomass, could be enhanced
400 by modifying the physical properties of a given suspensions. Although better energy
401 efficiency and more intense cavitation can be obtained when applying higher input power
402 in diluted suspension, energy and water expenses should be assessed together with the
403 sonochemical effects to obtain an overall optimization of the process.

404

405 **5. Acknowledgments**

406 Authors acknowledge the INIA-ERDF (RTA2015-00060-C04-02 and RTA2015-00060-
407 C04-03) from Spain and the São Paulo Research Foundation – FAPESP (Grant
408 2017/06518-2) and the Coordination for the Improvement of Higher Level Personnel –
409 CAPES (Grant 88881.132626/2016-01) from Brazil for the financial support.

410

411 **6. References**

412 [1] H. Chen, X. Fu, Industrial technologies for bioethanol production from lignocellulosic
413 biomass, *Renewable and Sustainable Energy Reviews*, 57 (2016) 468-478.

- 414 [2] C.R. Somerville, H. Youngs, H. Szemenyei, N. Sorek, T.H. Yeats, The Implications
415 of Lignocellulosic Biomass Chemical Composition for the Production of Advanced
416 Biofuels, *BioScience*, 64 (2014) 192-201.
- 417 [3] S.S. Hassan, G.A. Williams, A.K. Jaiswal, Emerging technologies for the pretreatment
418 of lignocellulosic biomass, *Bioresource Technology*, 262 (2018) 310-318.
- 419 [4] N. Akhtar, K. Gupta, D. Goyal, A. Goyal, Recent advances in pretreatment
420 technologies for efficient hydrolysis of lignocellulosic biomass, *Environmental
421 Progress & Sustainable Energy*, 35 (2016) 489-511.
- 422 [5] Z.M.A. Bundhoo, R. Mohee, Ultrasound-assisted biological conversion of biomass
423 and waste materials to biofuels: A review, *Ultrasonics Sonochemistry*, 40 (2018)
424 298-313.
- 425 [6] P.B. Subhedar, P.R. Gogate, Ultrasound-assisted bioethanol production from waste
426 newspaper, *Ultrasonics Sonochemistry*, 27 (2015) 37-45.
- 427 [7] R. Sindhu, P. Binod, A.K. Mathew, A. Abraham, E. Gnansounou, S.B. Ummalyma,
428 L. Thomas, A. Pandey, Development of a novel ultrasound-assisted alkali
429 pretreatment strategy for the production of bioethanol and xylanases from chili post
430 harvest residue, *Bioresource Technology*, 242 (2017) 146-151.
- 431 [8] M.S.U. Rehman, I. Kim, Y. Chisti, J.-I. Han, Use of ultrasound in the production of
432 bioethanol from lignocellulosic biomass, *Energy Education Science and
433 Technology Part A: Energy Science and Research*, 30 (2013) 1391-1410.
- 434 [9] M.A. Margulis, I.M. Margulis, Calorimetric method for measurement of acoustic
435 power absorbed in a volume of a liquid, *Ultrasonics Sonochemistry*, 10 (2003) 343-
436 345.
- 437 [10] J.A. Cárcel, J. Benedito, J. Bon, A. Mulet, High intensity ultrasound effects on meat
438 brining, *Meat Science*, 76 (2007) 611-619.

- 439 [11] T. Kikuchi, T. Uchida, Calorimetric method for measuring high ultrasonic power
440 using water as a heating material, *Journal of Physics: Conference Series*, 279 (2011)
441 012012.
- 442 [12] J. Berlan, T.J. Mason, Dosimetry for power ultrasound and sonochemistry, in: T.J.
443 Mason (Ed.) *Advances in Sonochemistry*, JAI Press Inc, Londres, 1996, pp. 1-73.
- 444 [13] J.-M. Löning, C. Horst, U. Hoffmann, Investigations on the energy conversion in
445 sonochemical processes, *Ultrasonics Sonochemistry*, 9 (2002) 169-179.
- 446 [14] P.R. Gogate, A.B. Pandit, Engineering design method for cavitation reactors: I.
447 Sonochemical reactors, *AIChE Journal*, 46 (2000) 372-379.
- 448 [15] J.A. Cárcel, J.V. García-Pérez, J. Benedito, A. Mulet, Food process innovation
449 through new technologies: Use of ultrasound, *Journal of Food Engineering*, 110
450 (2012) 200-207.
- 451 [16] P.R. Gogate, Application of cavitation reactors for water disinfection: Current
452 status and path forward, *Journal of Environmental Management*, 85 (2007) 801-
453 815.
- 454 [17] J. Raso, P. Manas, R. Pagan, F.J. Sala, Influence of different factors on the output
455 power transferred into medium by ultrasound, *Ultrasonics Sonochemistry*, 5 (1999)
456 157-162.
- 457 [18] T.A. Mamvura, S.E. Iyuke, A.E. Paterson, Energy changes during use of high-power
458 ultrasound on food grade surfaces, *South African Journal of Chemical Engineering*,
459 25 (2018) 62-73.
- 460 [19] T.C. Polachini, G.R.d. Carvalho, J. Telis-Romero, Determination of acoustic fields
461 in acidic suspensions of peanut shell during pretreatment with high-intensity
462 ultrasound, *Brazilian Journal of Chemical Engineering*, 34 (2017) 385-394.

- 463 [20] R.F. Contamine, A.M. Wilhelm, J. Berlan, H. Delmas, Power measurement in
464 sonochemistry, *Ultrasonics Sonochemistry*, 2 (1995) S43-S47.
- 465 [21] M. Toma, S. Fukutomi, Y. Asakura, S. Koda, A calorimetric study of energy
466 conversion efficiency of a sonochemical reactor at 500 kHz for organic solvents,
467 *Ultrasonics Sonochemistry*, 18 (2011) 197-208.
- 468 [22] J.H. Gibson, H. Hon, R. Farnood, I.G. Droppo, P. Seto, Effects of ultrasound on
469 suspended particles in municipal wastewater, *Water Research*, 43 (2009) 2251-
470 2259.
- 471 [23] H. Ferkous, O. Hamdaoui, S. Merouani, Sonochemical degradation of naphthol blue
472 black in water: Effect of operating parameters, *Ultrasonics Sonochemistry*, 26
473 (2015) 40-47.
- 474 [24] S. Gupta, D.L. Feke, Acoustically driven collection of suspended particles within
475 porous media, *Ultrasonics*, 35 (1997) 131-139.
- 476 [25] B. Saint-Michel, H. Bodiguel, S. Meeker, S. Manneville, Simultaneous
477 Concentration and Velocity Maps in Particle Suspensions under Shear from Rheo-
478 Ultrasonic Imaging, *Physical Review Applied*, 8 (2017) 014023.
- 479 [26] T.J. Mason, J.P. Lorimer, *Applied sonochemistry*, Wiley-vch, Weinheim, 2002.
- 480 [27] Y. Son, M. Lim, J. Khim, Investigation of acoustic cavitation energy in a large-scale
481 sonoreactor, *Ultrasonics Sonochemistry*, 16 (2009) 552-556.
- 482 [28] M.M. Chivate, A.B. Pandit, Quantification of cavitation intensity in fluid bulk,
483 *Ultrasonics Sonochemistry*, 2 (1995) S19-S25.
- 484 [29] C.K. McDonnell, J.G. Lyng, J.M. Arimi, P. Allen, The acceleration of pork curing
485 by power ultrasound: A pilot-scale production, *Innovative Food Science &*
486 *Emerging Technologies*, 26 (2014) 191-198.

487 [30] J.A. Cárcel, J. Benedito, C. Rosselló, A. Mulet, Influence of ultrasound intensity on
488 mass transfer in apple immersed in a sucrose solution, Journal of Food Engineering,
489 78 (2007) 472-479.
490
491